LBL-31475
Preprint

Lawrence Berkeley Laboratory
UNIVERSITY OF CALIFORNIA

Submitted to Physical Review C

The Nuclear Stopping Power at AGS Energies

S. Chapman and M. Gyulassy

November 1991

NUCLEAR SCIENCE DIVISION

LOAN COPY
Circulates
for 4 weeks
Bldg. 50 Library.
LBL-31475
Copy 2

Prepared for the U.S. Department of Energy under Contract Number DE-AC03-76SF00098

DISCLAIMER

This document was prepared as an account of work sponsored by the United States Government. Neither the United States Government nor any agency thereof, nor The Regents of the University of California, nor any of their employees, makes any warranty, express or implied, or assumes any legal liability or responsibility for the accuracy, completeness, or usefulness of any information, apparatus, product, or process disclosed, or represents that its use would not infringe privately owned rights. Reference herein to any specific commercial product, process, or service by its trade name, trademark, manufacturer, or otherwise, does not necessarily constitute or imply its endorsement, recommendation, or favoring by the United States Government or any agency thereof, or The Regents of the University of California. The views and opinions of authors expressed herein do not necessarily state or reflect those of the United States Government or any agency thereof or The Regents of the University of California and shall not be used for advertising or product endorsement purposes.

Lawrence Berkeley Laboratory is an equal opportunity employer.

DISCLAIMER

This document was prepared as an account of work sponsored by the United States Government. While this document is believed to contain correct information, neither the United States Government nor any agency thereof, nor the Regents of the University of California, nor any of their employees, makes any warranty, express or implied, or assumes any legal responsibility for the accuracy, completeness, or usefulness of any information, apparatus, product, or process disclosed, or represents that its use would not infringe privately owned rights. Reference herein to any specific commercial product, process, or service by its trade name, trademark, manufacturer, or otherwise, does not necessarily constitute or imply its endorsement, recommendation, or favoring by the United States Government or any agency thereof, or the Regents of the University of California. The views and opinions of authors expressed herein do not necessarily state or reflect those of the United States Government or any agency thereof or the Regents of the University of California.

LBL-31475

The Nuclear Stopping Power at AGS Energies*

Scott Chapman and Miklos Gyulassy

Nuclear Science Division
Lawrence Berkeley Laboratory
Berkeley, CA 94720 USA

November 6, 1991

Abstract

Fireball, firestreak and hadronic string models are shown to overpredict recent central 15 AGeV Si+Au E802 spectrometer data by at least 70%. Claims in the literature about full nuclear stopping in Si+Au reactions are therefore premature. In fact, fits to the spectrometer data indicate that up to half of the projectile nucleons may lose less than one unit of rapidity after traversing 5-10 fm of nuclear matter, implying possibly a surprisingly long stopping length of ~20 fm. Comparison of these same fits with E810, E814, and preliminary E802 $dN_{charged}/d\eta$ data suggests, however, that there may be some inconsistencies among the various data sets, and therefore that additional data will be needed to establish the degree of nuclear stopping at AGS energies.

PACS : 24.10.-i, 25.70.Np, 13.85.Ni

*This work was supported by the Director, Office of Energy Research, Division of Nuclear Physics of the Office of High Energy and Nuclear Physics of the U.S. Department of Energy under Contract No. DE-AC03-76SF00098.

1 Introduction

It is popularly believed that "full stopping is realized [1-4], showing a behavior close to the Landau model[5] and to relativistic fluid dynamics[6], and the energy density can reach values comparable to the critical values for QGP formation"[7]. However, as we pointed out in ref. [8], the published E802 spectrometer data[9] cast doubt on this belief, since in fact none of the present models is consistent with the full array of data. Moreover, unless the systematic errors of the spectrometer data are very large, these data are more indicative of a surprising degree of nuclear transparency. As we show below, however, no firm conclusion can be made on this important topic, since the data on $dN_{charged}/d\eta$[10] as well as those reported by E810[11] and E814[12] are not completely consistent. In this paper our aim is to clarify what are the problems at present in drawing conclusions about nuclear stopping power in these reactions.

In our letter[8] we discussed a model independent fit to the spectrometer data which implied that if systematic errors do not cause more than a 30% suppression of proton and pion yields, then 4-momentum and baryon conservation laws imply that at least 11 out of 28 projectile nucleons suffer less than one unit of rapidity loss during the collision. In this paper, we give the precise functional form of the fit used in the letter, as well as introducing three other fits which allow for the possibility of systematic errors in excess of 30%. In addition to E802 spectrometer data, we compare these four fits to E802 $dN_{charged}/d\eta$ data[10] as well as data from the E810[11] and E814[12] collaborations. In our letter, we developed a multicomponent model (mcm) in order to quantify the amount of nuclear stopping implied by the E802 spectrometer data. In this paper, in addition to explaining the mcm in more detail, we show that a simpler double firestreak model leads to similar conclusions about the amount of stopping. These types of models are only able to reproduce the spectrometer data with stopping lengths of ~20 fm. In addition to central Si+Au data, we discuss the agreement of these models with unpublished preliminary central Si+Al and Si+Cu E802 spectrometer data[13], and make predictions for central Au+Au proton and

pion distributions at these same energies. The long stopping lengths implied by the E802 spectrometer data provide a sharp contrast to the results of p+p and p+A experiments at these same energies which imply stopping lengths of more on the order of 8-10 fm[14]. Thus, either something new and unexplained is occurring in central Si+Au collisions at the AGS, or else the systematic errors of the spectrometer data are larger than reported. In any case, the E802 spectrometer data do not support the claims of full nuclear stopping which are so prevalent in the literature [1-5,7,15-18].

2 The Hadronic Fireball

In the generic hadronic fireball model[19], the projectile nucleus is assumed to be completely stopped by the target nucleus in the participant center-of-mass frame, whereupon thermal and chemical equilibrium are established. By treating both nuclei as hard spheres of constant baryon density ($\rho_0 = .145 fm^{-3}$), geometry determines the number of interacting nucleons for any given impact parameter. For example, in a b=0 Si+Au collision, all 28 ($= N_p$) silicon nucleons interact with a central tube of about 75 ($= N_t$) gold nucleons, thus making the baryon number of the resulting fireball 103 ($= N_f$). The remaining 122 gold nucleons of this example are merely spectators which are ignored in this model. Once N_p and N_t are known, the rapidity of the fireball rest frame and the total fireball energy in that frame are fixed by kinematics. For the Si+Au example with $y_{p0} = 3.4$ and $y_{t0} = 0$, $y_f = 1.3$ and $E_f =$ 250GeV.

After its creation, the fireball expands and cools until freezeout, when the mean free path of the fireball hadrons becomes approximately the same size as the radius of the fireball. The temperature and chemical potentials at freezeout define the particle distributions according to

$$f_i = \frac{dN_i}{dy d^2p_\perp} = \frac{\gamma_i g_i V_{fr} E}{\exp\{(E - B_i\mu - S_i\mu_s)/T\} - (-1)^{B_i}} \tag{1}$$

where B_i, S_i and g_i are the baryon number, strangeness, and spin-isospin multiplicity

for each species of hadron, V_{fr} is the freezeout volume, and γ_i is a parameter introduced to allow for incomplete the chemical equilibration. We assume that $\gamma_i = \gamma_s$ for all strange hadrons and $\gamma_i = 1$ for all other hadrons. Since E_f and N_f are fixed by kinematics, T, μ and μ_s can be found by choosing values for γ_s and V_{fr} (or $\rho_{fr} = N_f/V_{fr}$) and then solving the following integral equations:

$$E_f = \sum_{i=hadrons} \int d^2p_\perp dy E f_i \tag{2}$$

$$N_f = \sum_{i=baryons} B_i \int d^2p_\perp dy f_i \tag{3}$$

$$0 = \sum_{\substack{strange \\ i=hadrons}} S_i \int d^2p_\perp dy f_i \tag{4}$$

We treat explicitly only the following hadronic resonances: N, Δ, Λ, Σ, π, η, ρ, ω, η', K, K^* and their antiparticles. For example, for $b = 0$, $\gamma_s = .5$ and $\rho_{fr} = 5\rho_0$, we find that T = 200 MeV, $\mu = 418$ MeV and $\mu_s = 92$ MeV for AGS energy.

Once T, μ and μ_s have been found for a given set of input parameters, $f_i(y, p_\perp)$ determine the invariant distributions for each species of hadron in the fireball. However, before reaching the detector, the heavy baryon and meson resonances decay as follows: $\Delta \to N+\pi$, $\Lambda \to p+\pi^-$(64% of the time), $\Sigma^+ \to p+\pi^0$ (52%), $\Sigma^+ \to n+\pi^+$ (48%), $\Sigma^0 \to p+\pi^-$ (64%), $\Sigma^- \to n+\pi^-$, $\eta \to 3\pi$(30%), $\rho \to 2\pi$, $\omega \to 3\pi$(90%), $\eta' \to 2\pi$, and $K^* \to K+\pi$, where the balance of the Λ, Σ^0, η and ω decays are into undetected neutrals. For the 3π decays, it is assumed for simplicity that each daughter particle carries away 1/3 of the parent energy. By convoluting the above decays with parent distribution functions as in ref. [20], the resonance contributions to the nucleon and pion distributions are found.

The net charge/baryon of the fireball is given by

$$(Z/A)_f = \frac{(Z_p/A_p)N_p + (Z_t/A_t)N_t}{N_f} \quad , \tag{5}$$

where Z_p (Z_t) and A_p (A_t) are the charge and atomic number of the projectile (target) nucleus. Charge conservation is enforced as follows: All final state mesons not coming from strange baryon decays are assumed to be distributed isosymmetrically, and therefore the net charge carried by these mesons is determined solely by the kaon abundances:

$$C_{mes} = N_{K^+} - N_{K^-} \tag{6}$$

From isosymmetry ($N_{K^0} = N_{K^+}$, etc.) and conservation of strangeness before strange baryon decays, we have the relation $C_{mes} = .5Y$, where Y is the number of strange baryons in the fireball. It is assumed that all of the strange baryons have the same mass (1.17 GeV) so that their relative abundances before decay do not depend on the temperature or chemical potentials. These abundances are taken to be 1/4, $1/2(Z/A)_f$, 1/4, and $1/2(1-(Z/A)_f)$ for Λ, Σ^+, Σ^0, and Σ^- respectively. In this way, the net charge/baryon of all strange hadrons is always identical to the incoming charge/baryon ratio of $(Z/A)_f$. If, on the other hand, we had chosen Λ's and Σ's to have different masses, we would either need to introduce another chemical potential or some more complicated prescription for choosing strange baryon abundances in order to enforce charge conservation for arbitrary T, μ and μ_s. Finally, by demanding that $(Z/A)_f$ of the final nucleons not coming from strange baryon decays be protons, overall charge conservation can be enforced.

In the E802 experiment, central Si+Au events were identified by a high multiplicity trigger whose cross section ($=\sigma_{cent}$) represented 7% of the total Si+Au inelastic cross section (=3822mb[13]). In our model, we chose a maximum impact parameter ($b_{max} = 2.9fm$) such that $\pi b_{max}^2 = \sigma_{cent}$ and then integrated our fireball results over b from 0 to b_{max}.

In the experiment, measurements were made using a spectrometer arm with a range of $5° < \theta < 55°$ which could detect and identify charged particles with total momentum between 0.5 and 3 GeV/c[9, 21]. The resulting raw particle distributions were binned both in y and $m_\perp$. For each rapidity bin, the distributions appear to be

well fit by pure exponentials in $m_\perp$[9]:

$$dN_i/dyd^2m_\perp = \rho_i(y)\exp(-(m_{i\perp} - m_i)/T_i(y)) \tag{7}$$

The rapidity distributions were then estimated by integrating these fits over $m_\perp$:

$$dN_i/dy = 2\pi\rho_i(y)T_i(y)(T_i(y) + m_i). \tag{8}$$

In the fireball model, dN_i/dy can be calculated in two ways: by numerically integrating f_i over all $d^2m_\perp$ or by using the exponential fitting procedure outlined above after imposing the experimental phase space constraints. For all of our calculations, the difference between the results of these two methods was less than 20% for dN_π/dy and completely negligible for dN_p/dy.

The solid line in fig. 1 shows the results of the generic fireball model outlined above with $\rho_{fr} = 5\rho_0$ and $\gamma_s = .5$. This fireball model produces more than a factor of 2 too many protons, pions, and kaons (not shown) at mid-rapidity. Using a higher freezeout baryon density results in more heavy baryon resonances and slightly fewer pions, but the increased temperature makes the distributions become too broad in $m_\perp$. Increasing (decreasing) γ_s increases (decreases) the number of kaons and strange baryons but does not have a significant effect on the total number of mid-rapidity protons and pions. In fact, no reasonable variation of ρ_{fr} and/or γ_s significantly improves agreement with the data. In addition to the generic fireball, fig. 1 also shows results from the Landau hydrodynamic longitudinally expanding fireball[5] (dashed line) and the hydrochemical spherically expanding fireball[17, 18] (dot-dashed line). The longitudinal expansion of the Landau fireball results in reduced proton and pion peaks at midrapidity. This expansion, however, only shifts the problem to higher rapidities, where again the model produces a factor of 2 more protons than are seen in the data. Even though the spherical expansion of the hydrochemical model provides a possible explanation for the difference in proton and pion slopes, the model again fails to reproduce the measured norms of these distributions. In fact, all of the

fireball models considered here overpredict the measured proton and/or pion rapidity distributions by about a factor of 2.

It has been suggested[17, 18] that at least some of the discrepancy in dN_π/dy could be due to an unmeasured excess of low-$p_\perp$ pions coming from baryon resonance decays. The dot-dot-dashed curves in the bottom two panels of figure 1 show the distributions of protons and pions coming only from baryon resonance decays in the generic fireball model. At least for the generic fireball, any low $p_\perp$ enhancement due to these resonances is entirely negligible for protons and less than 20% for pions, as can be seen by comparing the restricted, exponentially fitted dN_π/dy (dot-dot-dashed line in fig. 1) with the directly calculated dN_π/dy (solid line). Furthermore, even if one makes the assumption of the hydrochemical model[17, 18] that none of the pions coming from baryon resonance decays are detected, fireball models still predict 70% more mid-rapidity pions than are seen in the data (dashed line in fig. 1). Since none of the fireball models discussed here can reproduce the E802 data, we turn to other models.

3 The Firestreak and String Models

The firestreak[19, 22] model was designed to take into account the diffuse edges of colliding nuclei by creating many smaller scale regions of local equilibrium rather than a single large fireball. In this model, the projectile and target nuclei are divided into longitudinal tubes with transverse area $a_\perp(\lesssim 1fm^2)$. Each set of two opposing tubes forms a completely stopped miniature fireball (or firestreak) in its local center of mass frame. In this way a large number of independent firestreaks forms, each with its own local values of N_f, y_f, T, μ and μ_s. As a result of this locality, Wood-Saxon density distributions rather than sharp spheres can be used to determine how many nucleons are in each tube. Often, some very asymmetric cases will result. For example, a tube containing 3 nucleons from the center of a gold nucleus could interact

with a tube containing .1 nucleon from the diffuse edge of a projectile silicon nucleus to create a streak with $N_f = 3.1$ and $y_f = 0.4$. These asymmetries provide a natural way to generate low-rapidity "spectator" contributions, even though there are no true spectators in this model.

Hadronic string models[23] also feature locality, though they do not impose the requirement of complete nuclear stopping. In fig. 2, we compare the firestreak and two string models (Attila[24] and RQMD[15]) with the data. For the Firestreak and Attila, we have calculated $T_i(y)$ via the exponential fitting procedure of eqn. (7) in order to compare our curves to the published $T_i(y)$ values. Though the firestreak improves on the fireball by showing "spectator" contributions, it still has the problem of predicting far too many mid-rapidity protons and pions, even after the experimental acceptance has been folded in (dot-dot-dashed line in dN_π/dy). The string models do a better job of reproducing the overall ramp shape of dN_p/dy, though they overpredict the number of high rapidity protons by 50%. As for the pions, the string models again do better than the firestreak, though they still overpredict by 70% the dN_π/dy values reported by E802. Comparing Attila to RQMD shows that rescattering does not significantly improve the string model fits to the rapidity data. It should also be noted that the quark-gluon string model recently proposed in ref.[7] similarly overpredicts the number of mid-rapidity pions by at least 70%.

4 Model Independent Fits

Having seen that none of the above equilibrium and nonequilibrium models for nuclear collision dynamics are able to reproduce the published data, we consider next a model independent fitting procedure in order to isolate possible causes for the discrepancies. We begin by fitting the experimental $T_i(y)$[13] and $(dN/dy)_i(y)$[9] data with simple functions which have reasonable extrapolations to phase space regions outside of the experimental acceptance. Equations (7) and (8) are then used to determine the

invariant distributions, $f_i = dN_i/dyd^2m_\perp$, from which information about momentum and energy conservation can be extracted.

For the meson $(dN/dy)_i(y)$ we use

$$(dN/dy)_i = \alpha C_i exp(-(y-y_i)^2/\delta_i) \quad -1 \leq y \leq 4 \tag{9}$$

where $(C_i,\ y_i,\ \delta_i)$ are fit with (16, 1.4, 1), (16, 1.35, 1.3), (3.5, 0.95, 1) and (0.67, 1.3, 1) for π^+, π^-, K^+ and K^- respectively. The reported data is fit with $\alpha = 1$, but later we set $\alpha = 1.3$ to account for experimental systematic errors. The meson and proton temperatures are given by:

$$T_{\pi^+} = T_{\pi^-} = 0.06 + .1exp(-(y-1.3)^2/1.2) + 0.03exp(-y^2) \tag{10}$$

$$T_{K^+} = T_{K^-} = 0.19exp(-(y-1.3)^2/2.) \tag{11}$$

$$T_p = \begin{cases} 0.23exp(-(y-1.55)^2) + .1exp(-y^2) & y < 2.2 \\ 0.15 & y > 2.2 \end{cases} \tag{12}$$

We fit the proton rapidity spectrum with a falling quadratic ramp and include adjustable undetected spectator and projectile gaussians in order to conserve baryon number and to test for transparency:

$$(dN/dy)_p = \alpha \begin{cases} C_{spec}e^{(-y^2/\delta_{spec})} & -1 < y < 0 \\ Max\begin{bmatrix} C_{spec}e^{(-y^2/\delta_{spec})} \\ 6y^2 - 35y + 52 + C_{pro}e^{(-(y-y_{pro})^2/\delta_{pro})} \end{bmatrix} & 0 < y < 3 \\ 7 - 2y + C_{pro}e^{(-(y-y_{pro})^2/\delta_{pro})} & 3 < y < 3.5 \\ 0 & \text{otherwise} \end{cases} \tag{13}$$

where $\delta_{pro} = 0.25$. For the unobserved neutral mesons it is assumed that $\pi^0 = (\pi^+ + \pi^-)/2$, $K^0 = K^+$, and $\bar{K}^0 = K^-$. Charge conservation is enforced by demanding

that the total number of final protons be $N_p = 14 + 79 - N_{\pi^+} - N_{K^+} + N_{\pi^-} + N_{K^-}$ (= 91.9 for the above fit). For the case with no unexpected transparency ($C_{pro} = 0$), we use $C_{spec} = 85.5$ and $\delta_{spec} = 0.17$ in order to get the right value for N_p. With N_p fixed, the total number of undetected neutrons is given by baryon number conservation, $N_n = 28 + 197 - N_p = 133.1$. We assume that these are distributed in exactly the same was as the protons, i.e. $(dN/dy)_n(y) = (N_n/N_p)(dN/dy)_p(y)$. These fits allow us to take into account all of the observed energy in longitudinal and transverse motion as well as pion and kaon production. These fits are shown by the dashed lines in figs. 3 and 4 (solid lines for the temperatures).

The total outgoing longitudinal momentum P_z implied by these fits is easily calculated by integrating $m_\perp \sinh(y) f_i$ over $d^2m_\perp$ and y:

$$P_z = \sum_{i=hadrons} \int dy \frac{2T_i^2 + 2T_i m_i + m_i^2}{T_i + m_i} (dN/dy)_i \sinh(y) \quad . \tag{14}$$

E is simply found by replacing sinh(y) by cosh(y). With $C_{pro} = 0$ the integration over y gives $P_z = 241$ GeV/c and E = 455 GeV, whereas the total incoming energy and momentum are known to be $P_z = 409$ GeV/c (= 28 × 14.6) and E = 595 GeV (= 197 × .939 + 28 × 14.63). More than a third of the incoming momentum and a fourth of the energy are unaccounted for in these fits to the data! If we assume that neither leptons nor photons carry a significant fraction of the 4-momentum, then there must be some undetected hadrons somewhere which do carry it. The E802 collaboration has acknowledged that an undetected excess of low $p_\perp$ particles could result in a 25% normalization error of the dN/dy data[9]. To take into account these and/or other possible systematic errors in the data, we proceed by multiplying each of our $(dN/dy)_i$ functions by $\alpha = 1.3$ (adjusting C_{spec} to 48.6 for charge conservation) and find $P_z = 322$ GeV/c and E = 519 GeV. However, more than 85 GeV/c of momentum and 75 GeV of energy are still missing!

Either the systematic errors of the dN_i/dy data are significantly larger than 30%, or else the "missing" 4-momentum must be carried by an unexpectedly large number of undetected high-rapidity hadrons. The least transparent solution which does not

overpredict any of the data by more than 30% has (y_{pro}, C_{pro}, C_{spec}, δ_{spec}) = fit1 = (2.75, 3.4, 40.9, 0.17) and is shown by the solid lines in figs. 3 and 4. By allowing a 50% disagreement with the last proton data point, a slightly less transparent solution can be found: fit2 = (2.5, 4.29, 32.28, .25), as shown by the dot-dashed dN_p/dy in fig. 3. These solutions both have a neutron/proton ratio of 1.46 throughout and have 10.8 and 10.1 nucleons respectively in the projectile region ($2.44 < y < 3.5$). In the lower half of fig. 4 we show how an undetected low-$m_\perp$ component for pions could give rise to a 30% systematic error in dN_π/dy. However, since a high-$m_\perp$ hadron with rapidity y carries more 4-momentum than a low-$m_\perp$ hadron with the same rapidity, it is more conservative to use a uniform 30% enhancement everywhere as we did in our calculations.

Until now we have only discussed data from the E802 collaboration, but E810 has also taken data on 14.6 AGeV/c Si+Au collisions at the AGS[11]. The E810 TPC measures charged particle distributions using a central trigger which has approximately twice the cross-section of the E802 central trigger. This apparatus can distinguish between positively and negatively charged particles, but cannot identify their mass. Nevertheless, by assuming that all of the negatively charged particles are π^-'s, E810 is able to generate the π^- rapidity distribution shown by diamonds in fig. 3. It could be argued that we should not compare the E810 data with the E802 data since the E810 trigger is more peripheral. If we neglect this difference, however, the Gaussian fit of dN_{π^-}/dy can be widened by using $\delta_{\pi^-} = 1.85$ so that it agrees with the E810 negatives at high rapidities (dot-dashed dN_π/dy in fig. 3). By using fit3 = (2.5, 4.58, 72.7, 0.07) to define the proton distribution, 4-momentum can be conserved with 9.7 nucleons in the projectile region. The $y > 0$ protons in this fit are distributed almost identically to the protons in fit2, though from charge conservation the enhanced number of π^-'s causes a smaller n/p ratio (=1.33). Finally, from the fact that silicon is isosymmetric, one could argue that high-rapidity pions should be isosymmetric and therefore that the π^+'s should also be distributed like the E810 neg-

atives at high rapidities. This can be achieved by taking $\delta_{\pi^+} = 1.75$ and fit4 = (2.5, 1.92, 49.3, 0.09), which has only 6.6 nucleons in the projectile region and is shown by the dot-dot-dashed dN_p/dy and dN_π/dy curves in fig. 3. Though this fit conserves 4-momentum and displays closer to the expected amount of stopping, it disagrees with the last two π^+ data points by 70-100% and it features an n/p ratio of 1.56 even in the projectile region, where the pions were postulated to be isosymmetric.

It is instructive to compare the four fits discussed above to other preliminary data from E802 as well as to central Si+Pb data from experiment E814 at the AGS. In addition to the spectrometer arm, E802 has a target multiplicity array (TMA) detector which measures $dN/d\eta$ of charged particles and a beam calorimeter (ZCAL) which measures the residual beam energy after a collision. Due to the geometry of the ZCAL detector, there is some uncertainty as to whether it measures the energy of final particles with $\theta < 0.8°$ or with $\theta < 2.2°$[13]. For $\theta_{max} = 0.8°$ the four fits discussed above give ZCAL energies (in GeV) of (5.3, 3.8, 4.4, 4.1), while for $\theta_{max} = 2.2°$ these same fits give (37.0, 27.4, 30.6, 27.6). If θ_{max} is indeed 0.8°, then none of the above fits are inconsistent with correlations between the TMA (which defines the central trigger) and ZCAL measurements[13]. In fig. 5 we compare $dN/d\eta$ distributions from the four fits, the generic fireball, and the Attila[24] string model with preliminary TMA data[10] (The Landau fireball is compared with this same data in ref.[5] and RQMD is compared with it in ref.[16]). It is interesting that the four fits, each of which exceed the spectrometer multiplicities by at least 30%, still underestimate the TMA multiplicity. Attila, which over-predicts spectrometer pions by 70%, underestimates $dN/d\eta$ at low to mid pseudorapidities and overestimates $dN/d\eta$ at very high pseudorapidities. Only the fireball, which overestimates all spectrometer data by a factor of 2 at mid-rapidities, exceeds the measured peak of $dN/d\eta$ Since the TMA data has already been corrected for electron contributions and target thickness, it is difficult to resolve the apparent contradictions between the preliminary TMA multiplicities and the spectrometer data.

In the E814 experiment, neutrons emerging from Si+Pb collisions with a beam angle of $\theta < 0.8°$ are measured using a forward spectrometer[12]. Their rapidity is determined by the amount of energy that they deposit in the spectrometer, and so a dN_θ/dy plot of neutrons having $\theta < 0.8°$ is generated. In fig. 6 we compare dN_θ/dy from our four fits with leading neutron data for central ($\sigma \approx 40$mb) Si+Pb collisions[12]. The agreement is best for fit4, but due to the statistical uncertainty of the data as well as the different target (Pb) and trigger used by E814, none of the fits can be ruled out. In addition to leading neutrons, E814 also measures $dE/d\theta$[25]. Though this data is not yet published, we have plotted $dE/d\theta$ predictions for our four fits and Attila in fig. 7. It will be very interesting to see how the E814 data compares to these predictions, since for $5° < \theta < 15°$ $dE/d\theta$ is sensitive to the differences in the projectile region between the Attila model and our model independent fits.

It should be emphasized that the four fits are conservative in that each assumes that all of the E802 spectrometer data are systematically low by at least 30%. There are, of course, other solutions which are consistent both with the spectrometer data and with conservation laws. For example, abnormally large numbers of π^0's, photons, or high-energy electrons could be produced in these collisions without being detected by the spectrometer; however, these solutions imply bizarre and unprecedented physics. The four fits discussed above are thus the least unusual solutions which are consistent with the reported E802 spectrometer data. One might argue that simplest solution of all is that the spectrometer data are systematically low by 70%. In that case, most of the conventional models would be able to reproduce both the spectrometer dN/dy and the TMA $dN/d\eta$ data reasonably well. If these data do in fact have such large systematic errors for central Si+Au collisions, then one might expect these errors to also be present in central Si+Al collisions. However, in his Ph.D. thesis, Matt Bloomer performed an analysis using symmetric functions in which he found that energy conservation together with ZCAL data implied that systematic errors of the spectrometer data were less than 20% for central Si+Al

collisions[13]. We are led to conclude either that new systematic errors are present in central Si+Au collisions or that some new and unexpected physics occurs (i.e. anomalously large neutral particle production, or large numbers of final particles in the projectile region).

For the remainder of this paper, we assume that the normalization of the E802 spectrometer data is correct, and consequently that there are a large number of final nucleons in the projectile region due to an unexpectedly large amount of nuclear transparency in central Si+Au reactions. None of the models which we have considered in this paper feature the transparency necessary to reproduce this data, so none of them can make quantitative statements about stopping power of nuclei which are supported by the published E802 spectrometer data. Since the discrepancies between the models and the data are already at the 70% level for central Si+Au, there is no reason to believe that these models will be able to predict the behavior of Au+Au reactions to any better accuracy.

5 The Double Firestreak

The most straight-forward way to generalize the firestreak model to incorporate transparency is to assume that each tube-tube interaction produces two firestreaks (projectile and target) rather than one. We must then determine the rapidity (y_i) and rest energy per baryon (M_i^*) for each of these streaks. In order to treat projectile and target consistently, we must either pick y_p and y_t or M_p^* and M_t^*, since the remaining two can be solved for by energy and momentum conservation. A simple linear parametrization of the projectile and target streak rapidities is given by

$$y_p = y_{p0} - (\frac{N_t}{N_0})(\frac{\sigma_{in}}{a_\perp}) \quad and \quad y_t = (\frac{N_p}{N_0})(\frac{\sigma_{in}}{a_\perp}) \ , \tag{15}$$

where N_0 is the number of nucleons in a tube of size $a_\perp = \sigma_{in} = 30$mb necessary to cause a one unit rapidity shift of the opposing tube. The last factor in each of the above equations was included to insure that the stopping power would be

independent of the lattice size ($a_\perp$) chosen. Unfortunately, the above prescription leads to a number of cases where M^* of one of the fireballs is forced by 4-momentum conservation to be less than the mass of the nucleon. Fig. 8 shows the regions of (N_p, N_t) space for which this problem arises. Similar problems were encountered with other parametrizations in which y_p and y_t were chosen independently.

These problem regimes could in principle be handled specially by demanding complete transparency or the formation of a single fireball, but we chose instead to utilize a different algorithm which avoids special cases. First, in the center-of-mass frame of two colliding tubes containing N_p and N_t nucleons, the incoming momentum, P^*, is found. Next, the momentum of each tube is reduced by an amount proportional to the number of binary collisions, N_pN_t:

$$\Delta P^* = \delta p_z N_p N_t (\frac{\sigma_{in}}{a_\perp}) \tag{16}$$

Finally, the energy/baryon is required to be the same for both of the outgoing firestreaks ($M_p^* = M_t^* = M^*$). M^* and the CM firestreak rapidities y_p^* and y_t^* can then be found from the following equations:

$$M^* N_p sinh(y_p^*) = M^* N_t sinh(y_t^*) = P^* - \Delta P^* \tag{17}$$

$$M^* N_p cosh(y_p^*) + M^* N_t cosh(y_t^*) = M_{cm}(N_p + N_t) \ , \tag{18}$$

where the CM energy/baryon of the tube-tube system, M_{cm}, is determined by kinematics. Due to the symmetries of this method, M^* monatonically increases from m_N to M_{cm} as ΔP^* is increased from 0 to P^*. When the prescription of (16) gives a $\Delta P^* \geq P^*$, a single firestreak with $M^* = M_{cm}$ and $y_p^* = y_t^* = 0$ is assumed to be formed. Defining the effective nuclear thickness, z_i, via $N_i = a_\perp \rho_0 z_i$, the momentum shift per baryon of the projectile (target) is thus assumed to increase linearly with the effective target (projectile) thickness. The nuclear stopping power of this model is controlled by a single parameter–the momentum loss per binary collision δp_z, or equivalently, the nuclear stopping length

$$L_s = m_N \sinh(y_{p0}/2)/(\sigma_{in}\rho_0 \delta p_z) \ . \tag{19}$$

The meaning of this stopping length can be most easily seen in symmetric collisions ($z_p = z_t = z$), where the fractional momentum loss ($\Delta P^*/P^* = z/L_s$) increases linearly and reaches unity when $z = L_s$. Thus a stopping length of 10fm implies that two colliding tubes of length 10fm will just be able to stop each other.

In fig. 9 we compare models with various values of L_s to the data ($\rho_{fr} = 2\rho_0$ and $\gamma_s = 0.7$ have been chosen to provide the best agreement with kaon data and pion temperatures). Compared to the data, $L_s = 10$fm is evidently too small and $L_s = 26$fm is too large. Though $L_s = 17$fm provides good agreement to all but the last point of the dN_p/dy data, its pion peak is shifted to low rapidities, and its proton temperature is too low with a dip at midrapidity which is not seen in preliminary, unpublished $T_p(y)$ data[13]. This double firestreak description provides far better agreement with the data than any of the other models discussed so far, but in order to quantitatively reproduce all the features of the E802 data, further refinements are needed.

6 The Multicomponent Model

One of the key observations of E802 is that the transverse momentum slopes of protons and pions differ significantly. Therefore the amount of energy locked into transverse motion differs from that expected in simple thermal models with one freezeout temperature. Collective flow[17] provides one natural mechanism for different slopes. Different freezeout criteria due to different cross sections provides another. To test the effect of this difference on the conclusion of the stopping power, we introduce a more complex multicomponent model (mcm). We emphasize that this is not meant to be a realistic model of the physics, but a convenient numerical tool to help sort the implications of various features of the data.

We decompose a single fireball into two with two different freezeout times (one baryonic and one mesonic). Baryonic fireballs are assumed to consist of baryons

(no antibaryons), K^+'s and K^0's balanced such that they have zero net strangeness. Since the baryon resonances are allowed to decay as usual, there are some pions which are produced by baryonic fireballs. Mesonic fireballs are comprised of all hadronic resonances (including baryons), but have zero baryon number and strangeness. We suppose that each tube-tube collision gives rise to a fully stopped, double-freezeout firestreak at the local center of mass, in addition to receding projectile and target baryonic firestreaks. A number of new parameters must be introduced into this model to determine the energy and baryon number of each of the firestreaks involved.

First, as in the double firestreak, a value of L_s is specified in order to determine M^*, y_p^*, and y_t^* for the receding firestreaks. Second, another stopping length, L_s', is chosen in order to determine the fraction of baryons from each tube which get fully stopped:

$$f_s = (z_p z_t)^{1/2}/L_s' \ . \tag{20}$$

Next, if the initial CM energy/baryon, M_{cm}, of the tube-tube system is greater than an excitation mass parameter M_2^*, then the energy/baryon of the baryonic part of the central fireball is limited to $M_c^* = M_2^*$, and the energy/baryon available to the receding streaks becomes

$$M^* \rightarrow M^{*\prime} = \frac{1 - f_s(M_2^*/M_{cm})}{1 - f_s} M^* \tag{21}$$

in order to conserve energy. If, on the other hand, $M_{cm} \leq M_2^*$, then $M_c^* = M_{cm}$ and $M^{*\prime} = M^*$. If $M^{*\prime}$ turns out to be smaller than another parameter M_1^*, then there is no mesonic firestreak at all, and the tube-tube interaction is modeled by three purely baryonic streaks. However, if $M^{*\prime} > M_1^*$ then the receding streaks have their energy/baryon limited to M_1^* ($M_p^* = M_t^* = M_1^*$), and a mesonic streak overlapping the CM baryonic streak is created with energy

$$E_{mes} = (M^{*\prime} - M_1^*)(1 - f_s)(N_p cosh(y_p^*) + N_t cosh(y_t^*)) \ . \tag{22}$$

For the mesonic streaks, a freezeout temperature T_{mes} is specified and V_{fr} is solved for trivially, since $\mu = \mu_s = 0$ for streaks with zero baryon number and strangeness. Note

that if $(z_p z_t)^{1/2} \geq L'_s$ or $\Delta P^* \geq P^*((z_p z_t)^{1/2} \gtrsim L_s)$ for any two incoming tubes, then this model reduces to a fully-stopped firestreak with separate baryonic and mesonic freezeout criteria.

The many parameters of this model have interrelated effects but can be approximately explained as follows. The amount of baryon stopping is controlled by L_s and L'_s. The central ($1.1 < y < 1.7$) values of $T_p(y)$ are controlled by L'_s, M_2^*, and ρ_{fr}, while the wings ($y < 1.1$, $y > 1.7$) of $T_p(y)$ are controlled by M_1^* and ρ_{fr}. It should be noted that for baryonic firestreaks with M_i^* fixed, decreasing ρ_{fr} cools the baryons by forcing them into higher mass resonances. $T_\pi(y)$ is mainly controlled by T_{mes}, though ρ_{fr}, M_1^* and M_2^* also have effects by adjusting the number of cool pions coming from baryon resonances. The height of dN_π/dy is affected by all of the parameters; increasing the value of any one of them leads to a decrease in the number of pions. The overall number of kaons is adjusted by γ_s, while the K^+/K^- ratio is determined by the number of strange baryons, which is again a function of ρ_{fr}, M_1^* and M_2^*.

In figs. 10 and 11 we show various mcm solutions. The solid line is the best fit to the data (mcm1), with $L_s = L'_s = 26fm$, $M_1^* = 1.4$ GeV, $M_2^* = 1.85$ GeV, $\rho_{fr} = \rho_0$, $T_{mes} = 160$ MeV, and $\gamma_s = 0.25$. The dashed line (mcm2) was obtained by decreasing ρ_{fr} to $0.1\rho_0$, while the dot-dashed (mcm3) line was obtained by increasing M_1^*, M_2^* and T_{mes} to 1.55, 2 and .165 GeV respectively. The dot-dot-dashed curve is another fit to the data (mcm4) with $L_s = 20fm$, $L'_s = 50fm$, $M_1^* = 1.55$ GeV, $M_2^* = 2$ GeV, $\rho_{fr} = \rho_0$, $T_{mes} = 165$ MeV, and $\gamma_s = 0.25$. Due to the many adjustable parameters of this model, both mcm1 and mcm4 are able to quantitatively reproduce almost all of the E802 spectrometer data. The most notable discrepancy is the 50% overprediction of low rapidity pions by these models. Unlike the models discussed previously which also overpredict pions, the disagreement of the mcm fits is only seen at low rapidity, where the limited experimental $p_\perp$ acceptance has its largest effect[21]. In addition, by relaxing the assumption that neighboring streaks are thermally and chemically isolated from each other, some of the cool "spectator" streaks could "eat" pions from

their hotter neighbors. This effect would not be seen at higher rapidities where all of the streaks are hot. Both of the mcm fits as well as the $L_s = 17$ double firestreak exhibit the high degree of nuclear transparency necessary to be able to reproduce the E802 spectrometer data.

The $L_s = 17$ double firestreak as well as mcm1 and mcm4 discussed above have all had their parameters tuned to best fit the E802 central Si+Au spectrometer data. The quality of these fits is therefore not very surprising, especially in the case of the mcm where one has so many parameters to play with. A necessary test is to see how well these models can reproduce unpublished E802 central Si+Al and Si+Cu data[13]. For these reactions, there is very little difference between the results of mcm1 and mcm4; both of them are able to reproduce dN_π/dy and mid-rapidity dN_p/dy of both collisions to within 20%. Both parameter sets predict too many target protons, but this could be due to large fragment formation in these reactions. The $L_s = 17$ double firestreak obtains results similar to mcm1 and mcm2 for Si+Cu, but it exhibits a factor of 2 too few mid-rapidity protons and pions in central Si+Al collisions. Even though the double firestreak uses a smaller value for L_s than the mcm fits, it exhibits less stopping when applied to lighter nuclei. This is because there is no center-of-mass firestreak in the double firestreak model, so a lot of energy is carried away by receding mesons. This effect becomes much more pronounced with less stopping (lighter nuclei). It should be noted that we were not able to find a model which could simultaneously fit E802 p+A data and central A+B data. However, to the extent that central Au+Au reactions bear more similarity to central Si+A than to p+A reactions, the predictions for Au+Au by our mcm fits are better supported by the E802 spectrometer data than those of the models discussed in the first parts of this paper. In figure 14 we show Au+Au predictions by the $L_s = 10$ fm(dot-dot-dashed) and $L_s = 17$ fm (dot-dashed) double firestreaks as well as by the mcm fits (mcm1=solid, mcm2=short-dashed). For such large nuclei, the $L_s = 10$ fm double firestreak forms essentially a fully-stopped firestreak which consequently features a much narrower and higher peak in

dN_p/dy than the other models. This is due to the fact that full stopping has not been achieved in these models, as can be easily seen by looking at the long dashed line which represents the projectile proton rapidity distribution of mcml. Since Au+Au is symmetric, the projectile and target contributions combine to form a symmetric, gaussian-like dN_p/dy which would be difficult to differentiate from the result that one would get from a fully-stopped fireball undergoing longitudinal expansion. For asymmetric collisions like Si+Au, on the other hand, these two cases can be clearly distinguished. For this reason it is important to study and understand asymmetric as well as symmetric collisions.

7 Conclusion

We conclude that none of the present models which assume complete nuclear stopping and none of the present nonequilibrium string models are consistent with the published E802 spectrometer data for central Si+Au reactions. If the normalization error of the E802 data does not exceed 30%, then energy-momentum and baryon conservation alone require the existence of at least 11 nucleons in the projectile region ($y > 2.44$). Such a feature in the baryon spectrum would be indicative of a surprisingly high degree of nuclear transparency. A double firestreak and a multicomponent model have been developed to try to quantify the degree of transparency needed to reproduce the spectrometer data, and a nuclear stopping length of 17-26 fm was found. This length is much larger than the length of 8-10 fm which was expected based on other experiments at these and higher energies[14]. However, we emphasize here that there appears to be some discrepancy between the E802 spectrometer and other data sets. In particular, the $dN_{charged}/d\eta$[10] implies the existence of more charged particles at midrapidity than are seen by the spectrometer. Both $dN_{charged}/d\eta$ and the paucity of leading neutrons measured by E814[12] are more consistent with the amount of stopping predicted by a variety of conventional models. Therefore, new

data will be needed to resolve the issue of nuclear stopping at these energies.

Acknowledgements: We are especially grateful to Matt Bloomer, Shoji Nagamiya, Flemming Videbaek, Sam Lindenbaum and Johanna Stachel for extensive discussions on the AGS data.

References

[1] T. Abbott et al (E802 collab), Phys.Lett. B197 (1987) 285.

[2] M. S. Tannenbaum et al, Nucl. Phys. A488 (1988) 555c.

[3] P. Braun-Munzinger et al, Z. Phys. C38 (1988) 45.

[4] J. Stachel, Rapporteur's talk, PANIC XII, International Conference on Particles and Nuclei, MIT, 1990 (unpublished).

[5] J. Stachel, and P. Braun-Munzinger, Phys. Lett. B216 (1989) 1; Nucl. Phys. A498 (1989) 577c.

[6] E. F. Staubo et al, Phys. Lett. B229 (1989) 351.

[7] N. S. Amelin et al, Phys. Rev. C44 (1991) 1541.

[8] S. Chapman and M. Gyulassy, Phys. Rev. Lett. 67 (1991) 1210.

[9] T. Abbott et al (E802 collab), Phys. Rev. Lett. 64 (1990) 847; Phys. Rev. Lett. 66 (1991) 1567.

[10] F. Videbaek, Proceedings of the Workshop on Heavy Ion Physics at the AGS, March 5-7 (1990), ed. by Ole Hansen, p. 38. BNL-44911 and private communication with F. Videbaek.

[11] W. A. Love et al (E810 collab), Nucl. Phys. A525 (1991) 601c.

[12] J. Barrette et al (E814 collab), Phys. Rev. Lett. 64 (1990) 1219.

[13] M. A. Bloomer, MIT Ph.D thesis 1990 and private communication.

[14] W. Busza, R. Ledoux, Ann. Rev. Nucl. Part. Sci. (1988) 119; S. Date, M. Gyulassy, H. Sumiyoshi, Phys. Rev. D32 (1985) 619.

[15] H. Sorge et al, Nucl. Phys. A525 (1991) 95c; H. Sorge et al, UFTP preprint 263 (1991).

[16] R. Mattiello et al, Phys. Rev. Lett. 63 (1989) 1459.

[17] G. Brown et al, Phys. Rev. C43 (1991) 1881; C. M. Ko et al, Phys. Rev. Lett. 66 (1991) 2577.

[18] C. M. Ko et al, Erratum Phys. Rev. Lett. 67 (1991) 1811.

[19] J. Gosset, J. Kapusta, G. D. Westfall, Phys. Rev. C18 (1978) 844.

[20] S. Das Gupta and A. Z. Mekjian Phys. Rep. 72 (1981) 131-183.

[21] T. Abbott et al (E802 collab), Z. Phys. C. 38 (1988) 135.

[22] W. D. Myers, Nucl. Phys. A296 (1978) 177.

[23] B. Andersson, et. al., Nucl. Phys. B281 (1987) 289.

[24] M. Gyulassy, CERN-TH.4794 (1987), Proc. Balatonfured Conf. on Nuclear Physics (1987).

[25] D. Fox private communication.

Figure Captions

Figure 1. The upper panels show the proton and π^- rapidity distributions in 14.6 AGeV/c central $Si + Au$ reactions (solid dots), while the bottom panels show the $m_\perp$ distributions for $y = 1.3$ in these same reactions[9]. Solid curves show results of the generic fireball model, while dashed and dot-dashed curves denote Landau hydrodynamic fireball[5] and hydrochemical fireball[17, 18] results respectively. The norms of the hydrochemical results have been adjusted in accordance with the published erratum[18]. The dot-dot-dashed curves in the lower panels show $m_\perp$ distributions of protons and π^-'s coming only from heavy baryon decays in the generic fireball model. The dot-dot-dashed curve in the upper right panel shows the generic fireball prediction for the pion rapidity distribution given the restricted phase space of the experiment.

Figure 2. The top panels are as in Fig. 1, while the bottom panels are the inverse slope parameters of eqn. (7)[9]. These data are compared to firestreak[22] (dashed), Attila[24] (solid), and RQMD[15] (histogram) calculations. The dot-dot-dashed curve in the upper right panel shows the firestreak prediction with experimental phase space restrictions.

Figure 3. The same data as in Fig. 2, together with π^+ (solid) and E810 negatively charged particle (diamonds) data[11]. For clarity we show $dN_{\pi^+}/dy + 20$. The dashed curves in the upper panels as well as the solid curves in the lower panels are simple fits to the data. Also in the upper panels we show fit1 (solid), fit2 (dot-dashed protons and solid pions), fit3 (dot-dashed protons and π^- with solid π^+) and fit4 (dot-dot-dashed protons and π^+ with dot-dashed π^-).

Figure 4. The upper panels show the $K^{\pm}$ rapidity distributions in central $Si + Au$ reactions (solid dots), while the bottom panels show $m_{\perp}$ distributions for $y = 1.3$ in these same reactions[9]. Simple fits to the data are shown by dashed curves in the upper panels and solid lines in the lower panels. The solid curves in the upper panels show the 30% enhancement used in fit1 - fit4. The dashed line in the lower right panel shows a low $m_{\perp}$ component which would give rise to a 30% systematic error in dN_{π}/dy.

Figure 5. Preliminary $dN_{charged}/d\eta$ data[10] are compared to results of the generic fireball (long dashes), Attila (histogram), and model independent fits 1 (solid), 2 (dashed), 3 (dot-dashed), and 4 (dot-dot-dashed).

Figure 6. The histogram shows the rapidity distribution for neutrons emerging with a beam angle of less than 0.8° in central ($E_{\perp 814} > 13GeV$) Si+Pb collisions[12]. Fit1 (solid), fit2 (dashed), fit3 (dot-dashed), and fit4 (dot-dot-dashed) for central Si+Au are compared to this data.

Figure 7. Angular energy distributions (kinetic energy for baryons) are shown for Attila[24] (histogram), fit1 (solid), fit2 (dashed), fit3 (dot-dashed), and fit4 (dot-dot-dashed).

Figure 8. The available phase space for the stopping prescription of eqn. (15) is shown by the unshaded region. In the shaded region, one or both of the receding fireballs must have a mass/baryon $<$ .939 GeV in order to conserve 4-momentum.

Figure 9. Double firestreaks with L_s =10fm (dot-dashed), 17fm (solid), and 26fm

(dashed) are compared the data of fig. 2.

Figure 10. Multicomponent model fits mcm1 (solid), mcm2 (dashed), mcm3 (dot-dashed), and mcm4 (dot-dot-dashed) are compared to the data of fig. 2.

Figure 11. Multicomponent model fits mcm1 (solid), mcm2 (dashed), mcm3 (dot-dashed), and mcm4 (dot-dot-dashed) are compared to the data of fig. 4.

Figure 12. Predictions for central ($0 < b < 3$fm) Au+Au collisions by multicomponent model fits mcm1 (solid), mcm4 (dashed), and double firestreaks with L_s =10fm (dot-dot-dashed) and L_s =17fm (dot-dashed).

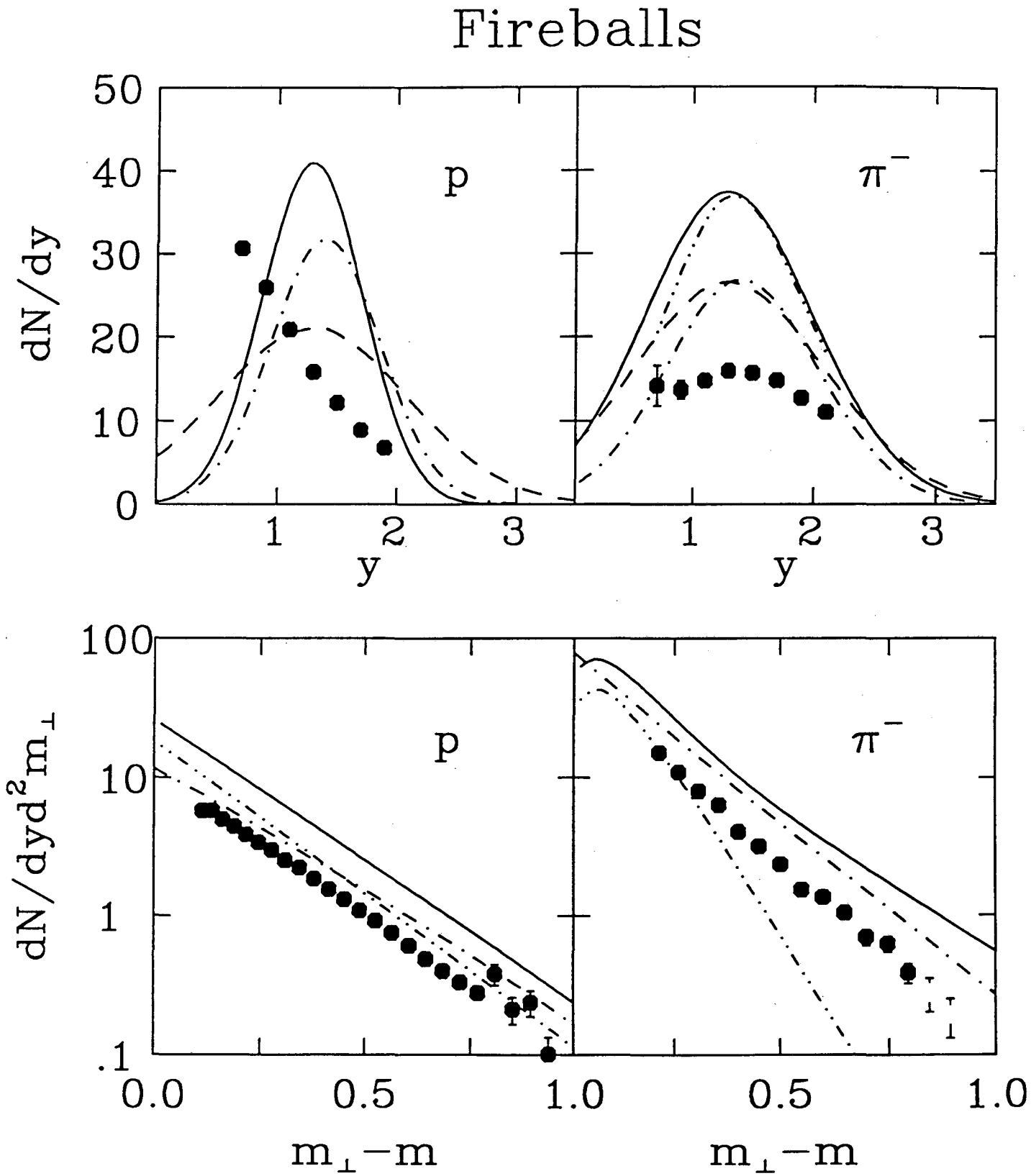
Fireballs
dN/dy
50
40
30
20
10
0
p
π⁻
1
2
3
y
dN/dyd²m⊥
100
10
1
.1
0.0
0.5
1.0
m⊥−m

Fig. 1 p. 25

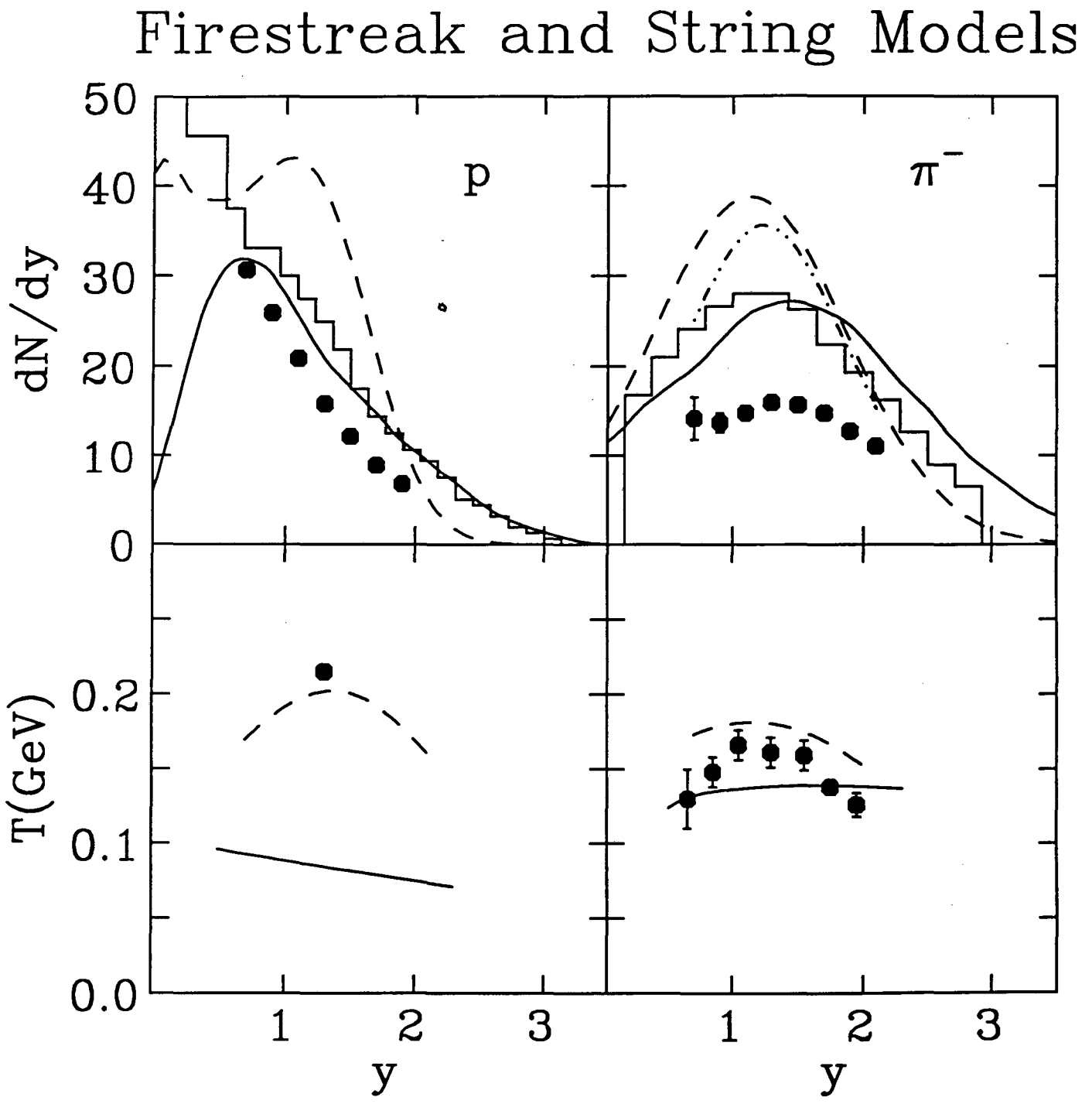
Firestreak and String Models
dN/dy
T(GeV)
p
π⁻
y
y
50
40
30
20
10
0
0.2
0.1
0.0
1
2
3
1
2
3

Fig. 2 p. 26

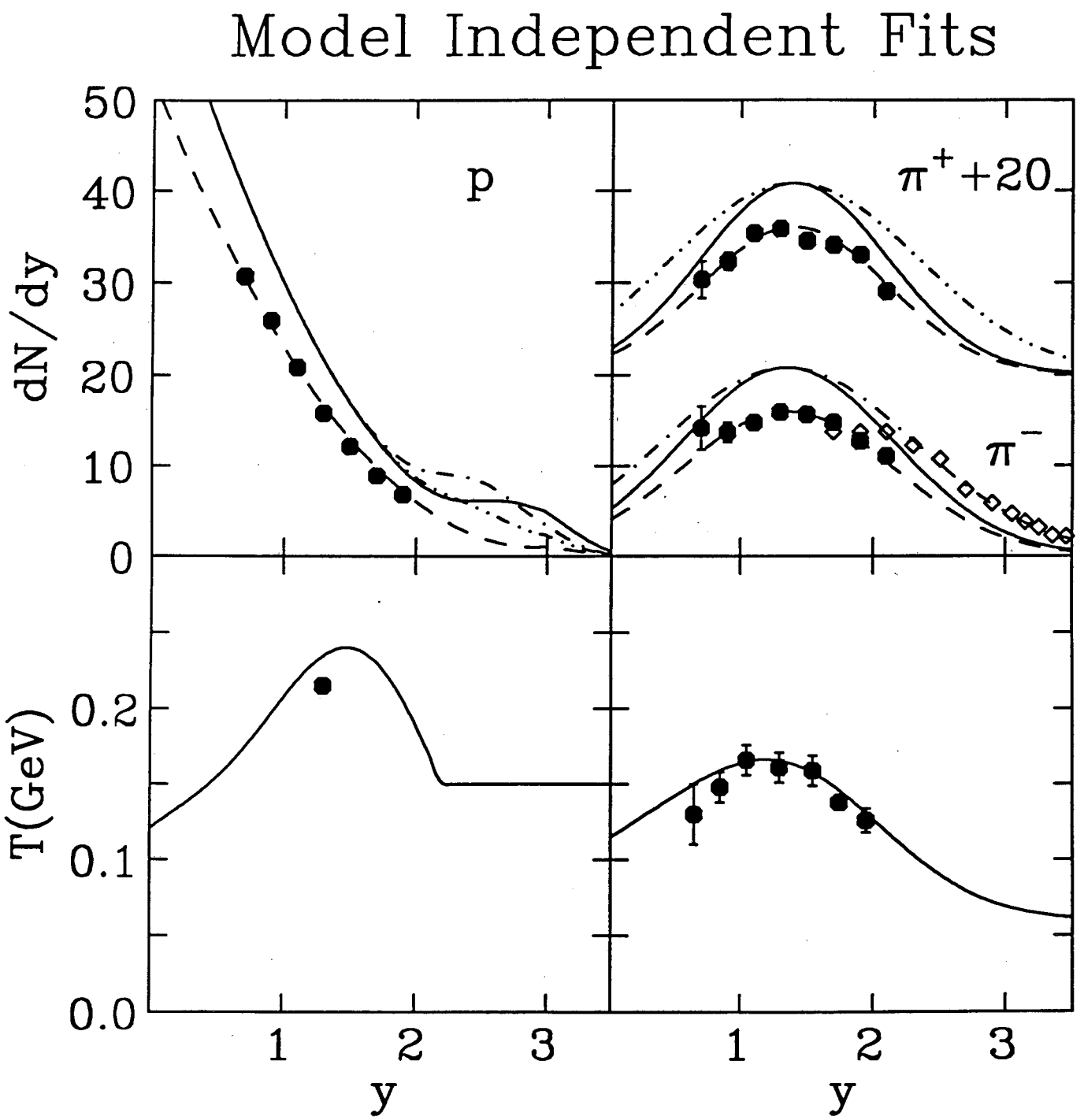
Model Independent Fits
dN/dy
T(GeV)
p
π^++20
π^-
y
y
50
40
30
20
10
0
0.2
0.1
0.0
1
2
3
1
2
3

Fig. 3 p. 27

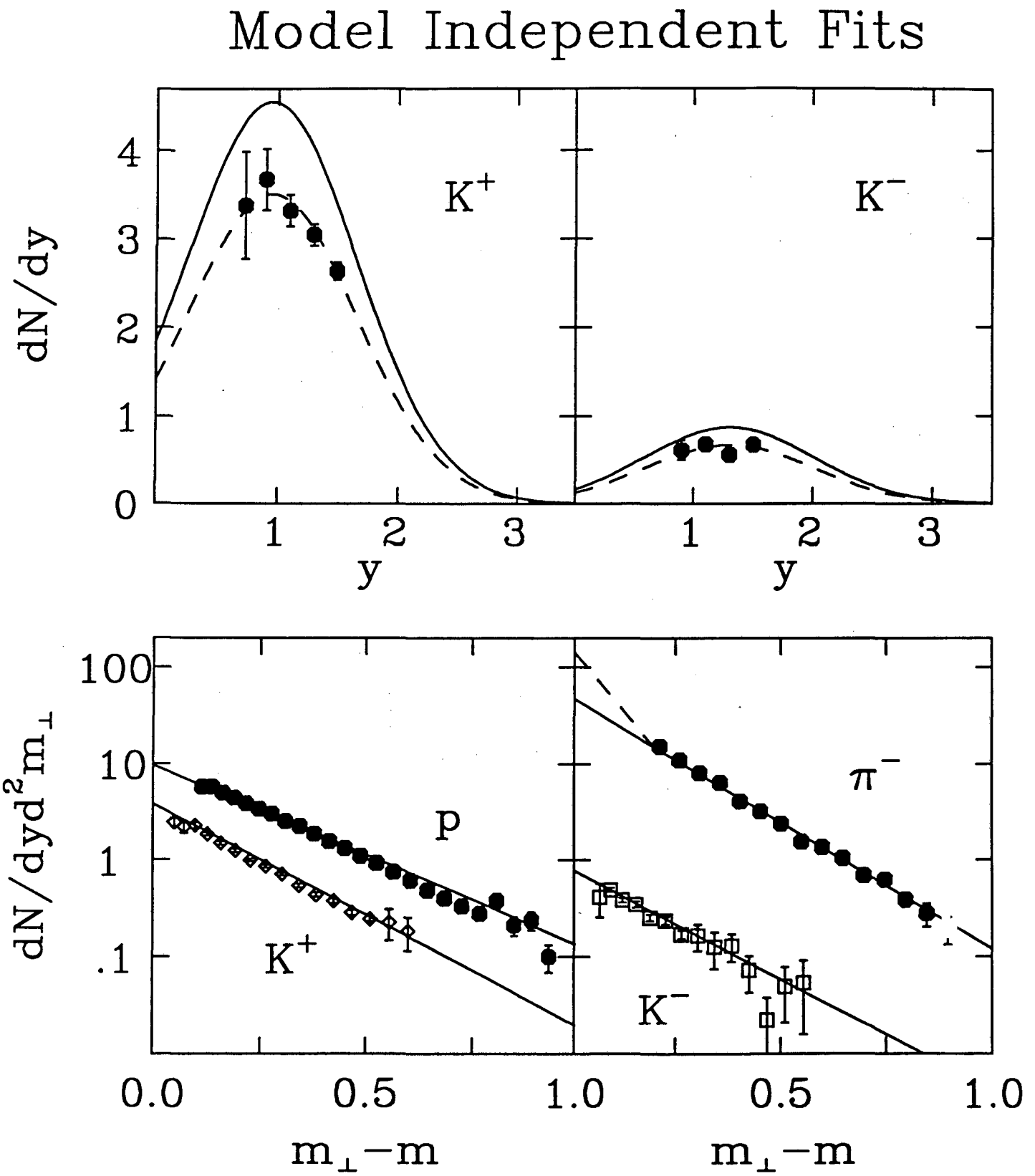

Fig. 4 p. 28

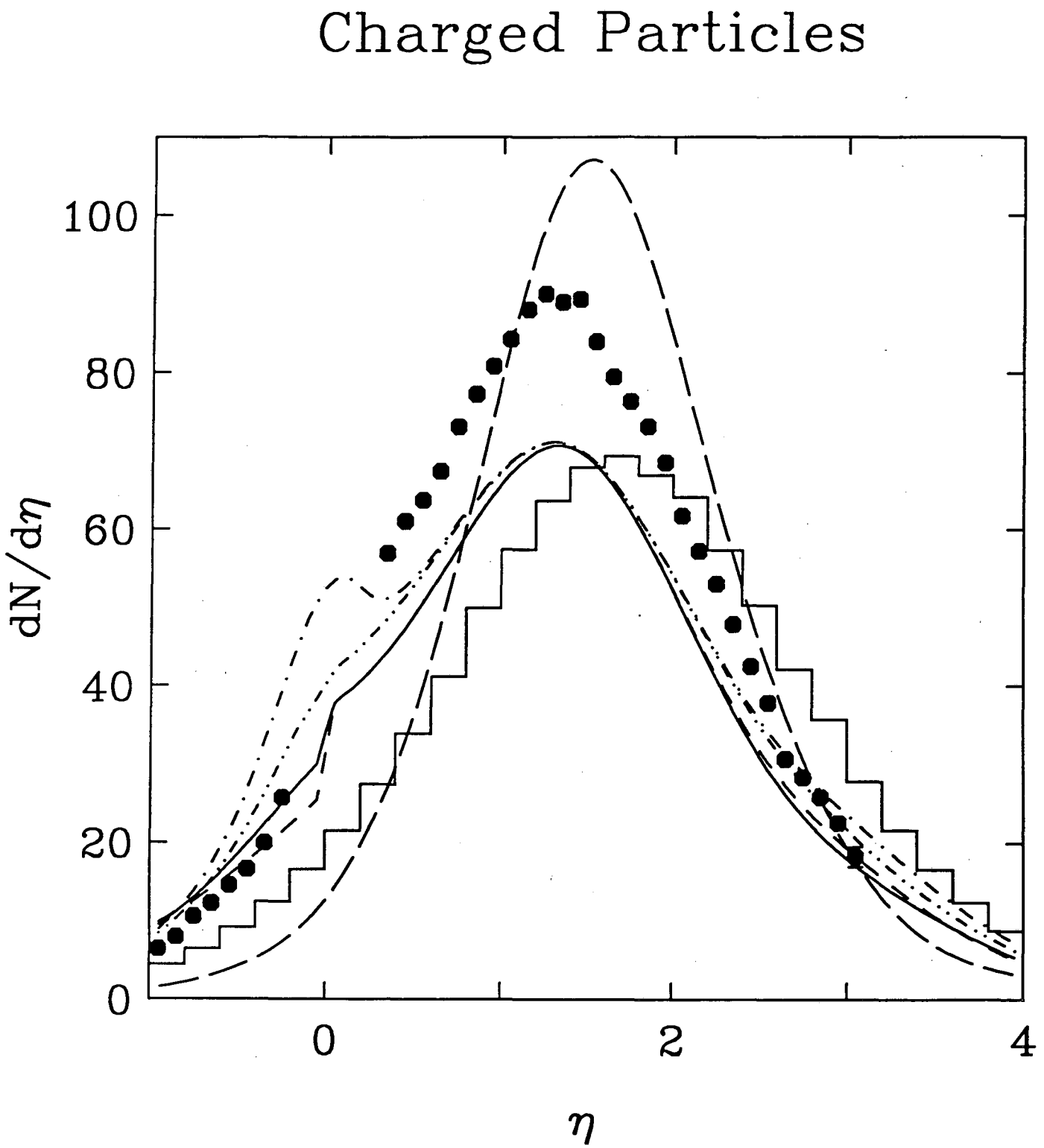

Fig. 5 p. 29

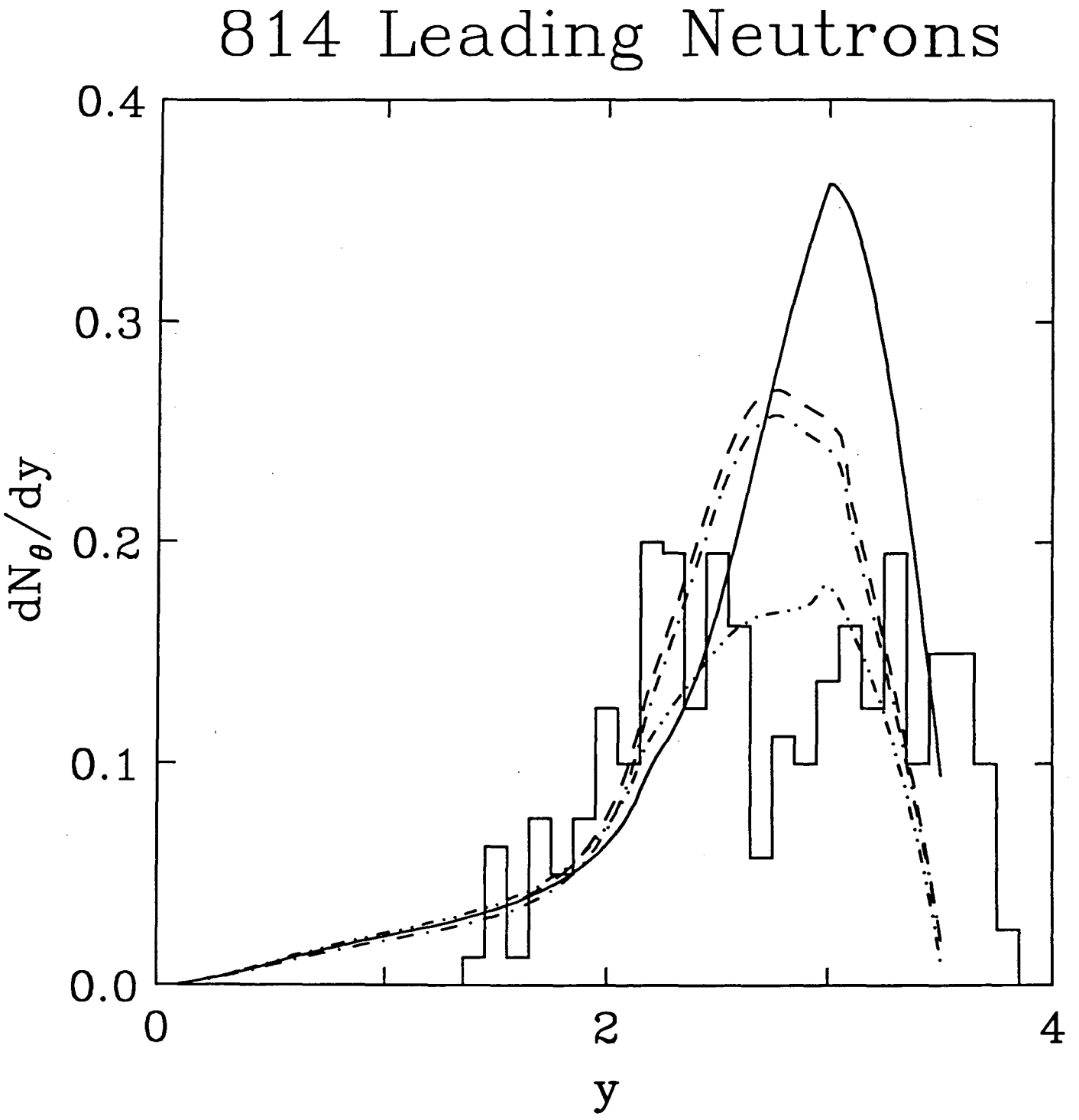

Fig. 6 p. 30

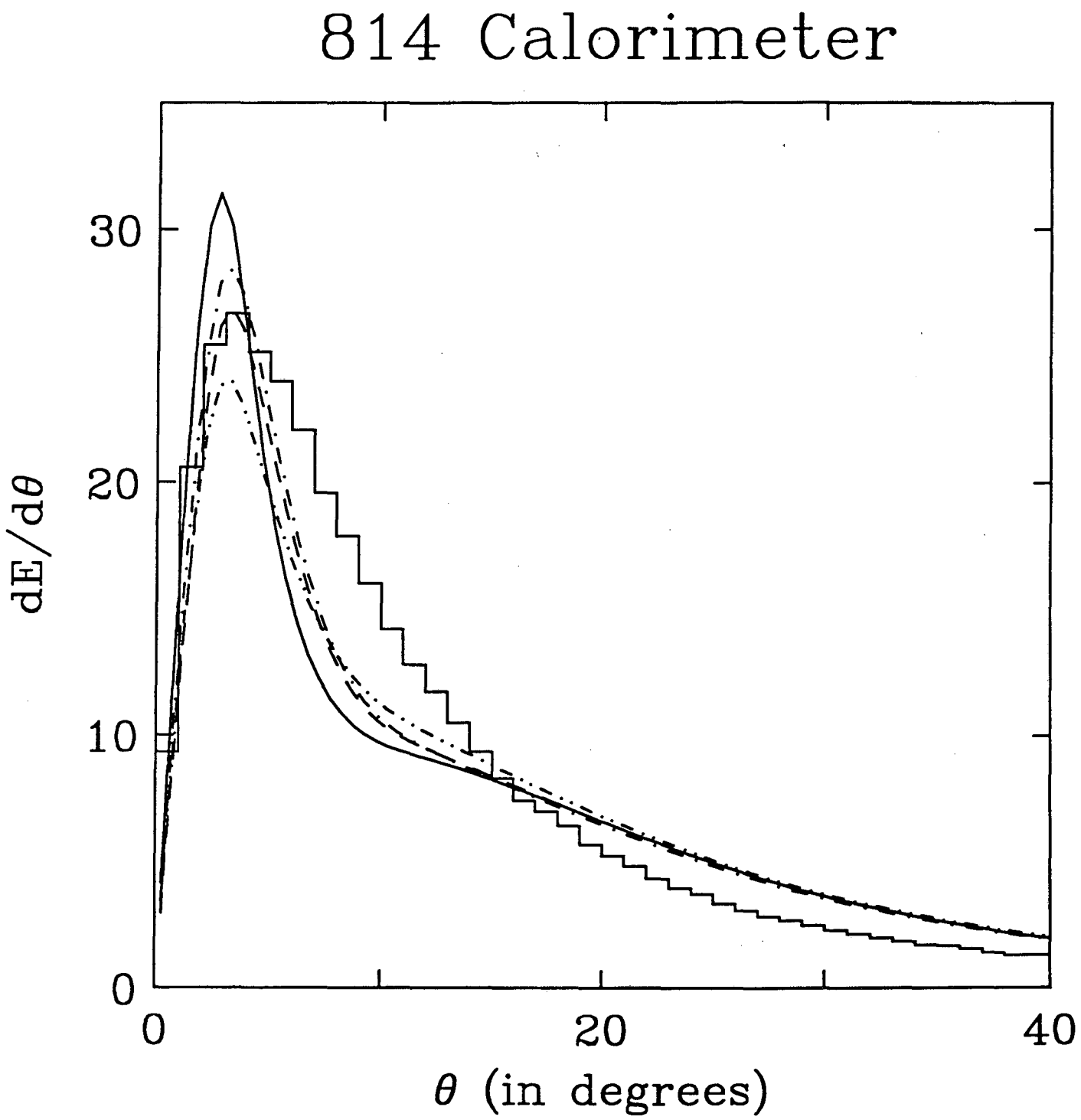
814 Calorimeter
30
20
10
0
dE/dθ
0
20
40
θ (in degrees)

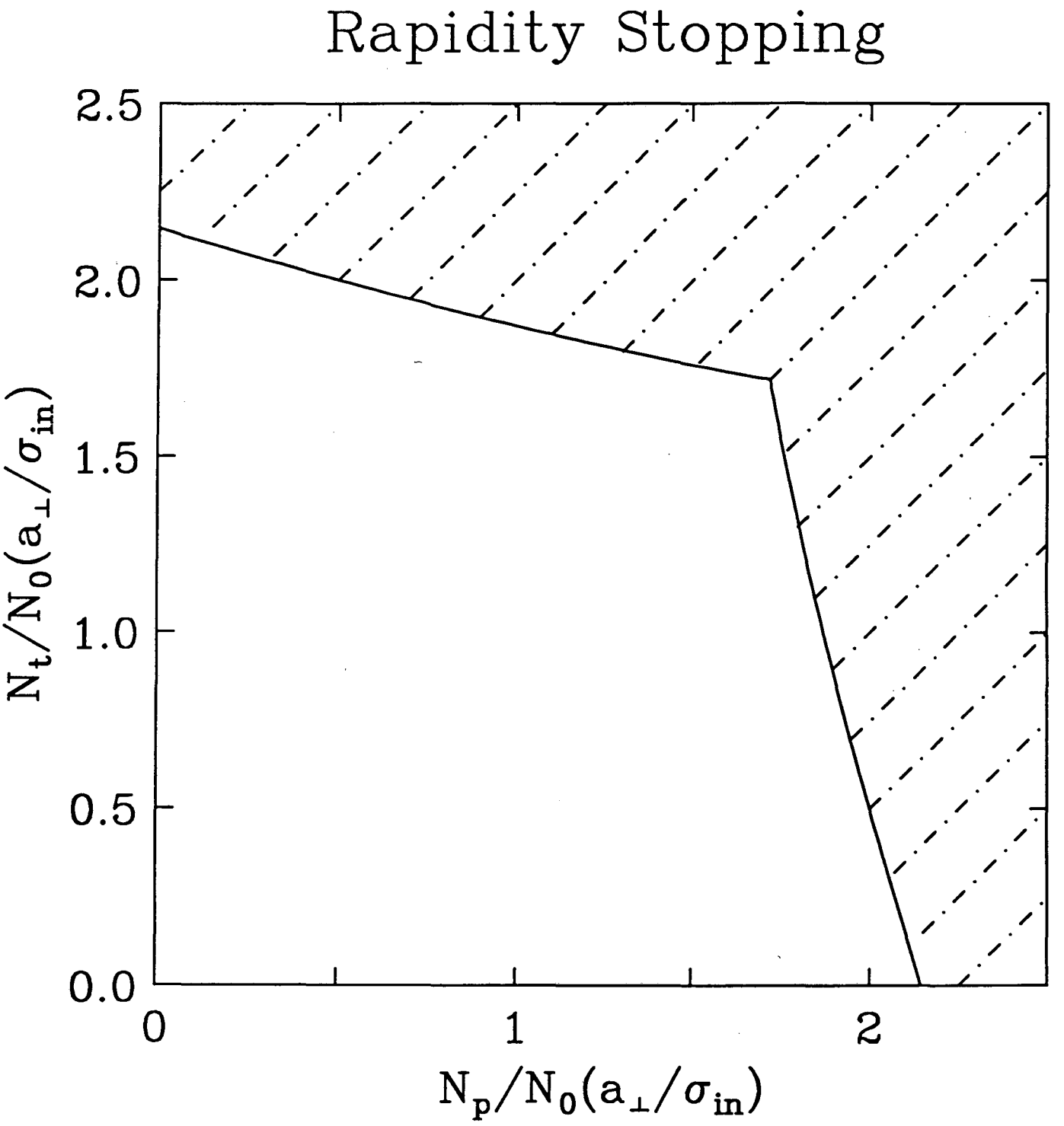
Rapidity Stopping
2.5
2.0
1.5
1.0
0.5
0.0
0
1
2
$N_t/N_0(a_\perp/\sigma_{in})$
$N_p/N_0(a_\perp/\sigma_{in})$

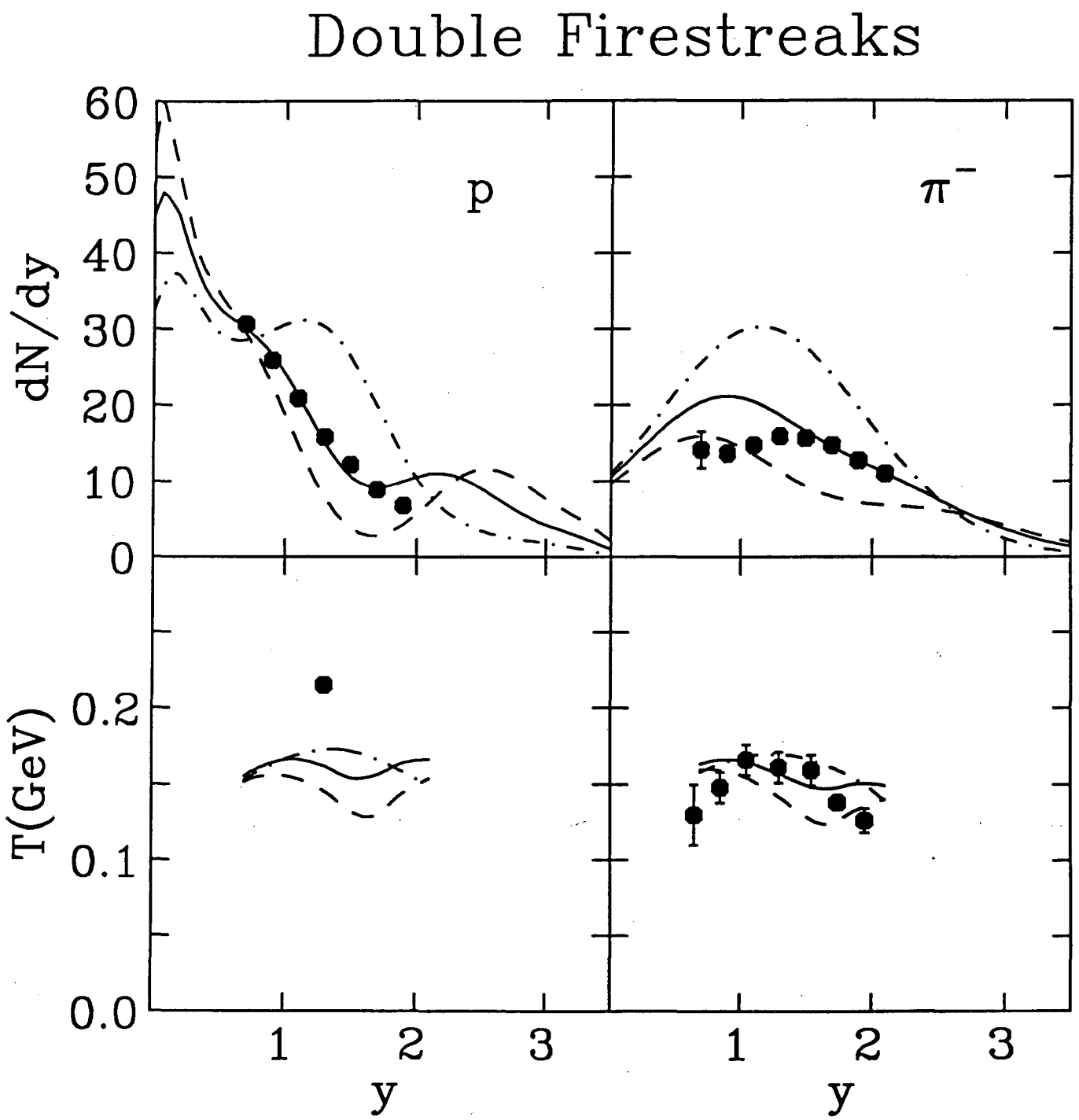
Double Firestreaks
p
π⁻
dN/dy
T(GeV)
y
y
60
50
40
30
20
10
0
0.2
0.1
0.0
1
2
3
1
2
3

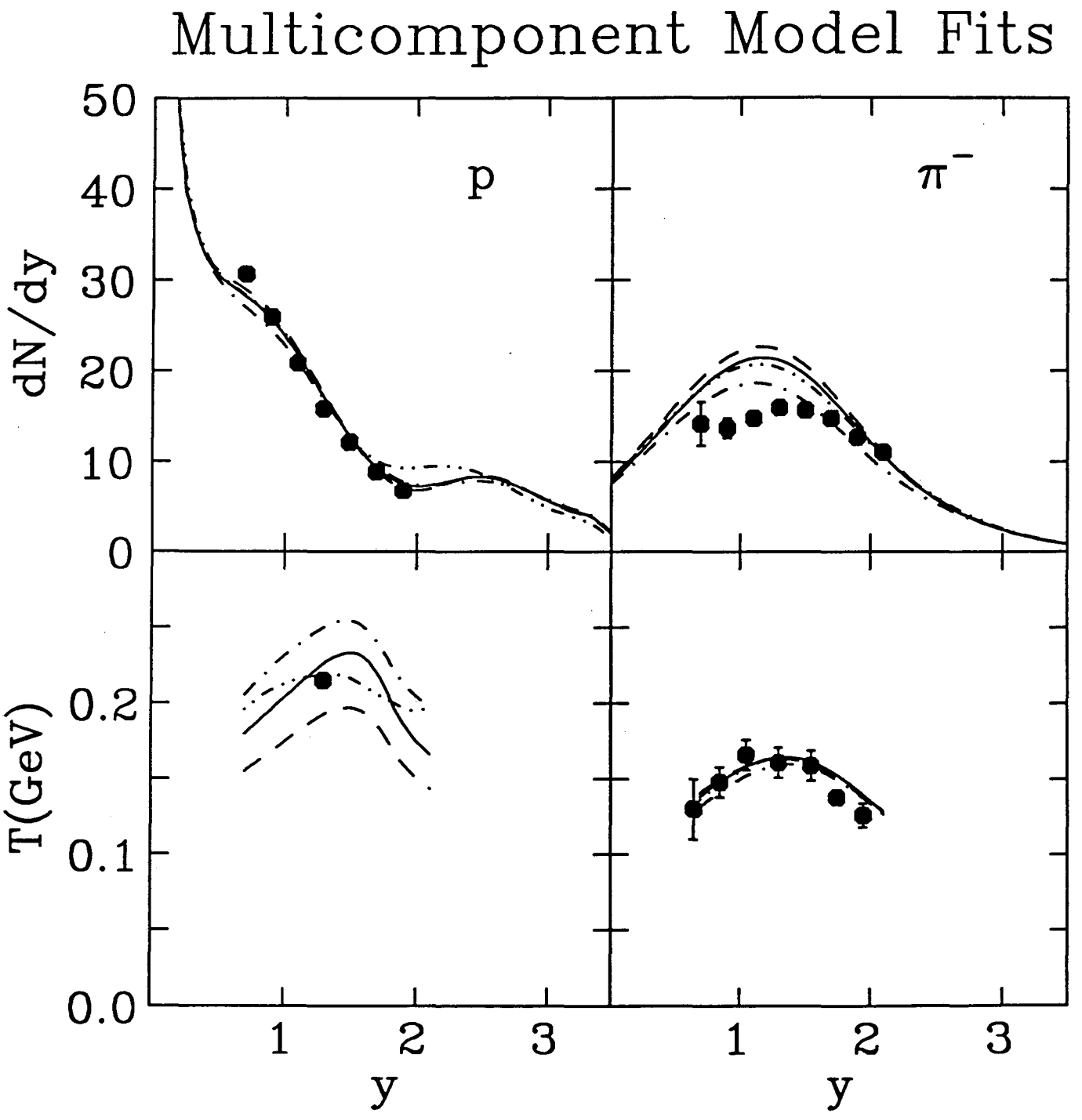
Multicomponent Model Fits
p
π^-
dN/dy
T(GeV)
y
y
50
40
30
20
10
0
0.2
0.1
0.0
1
2
3
1
2
3

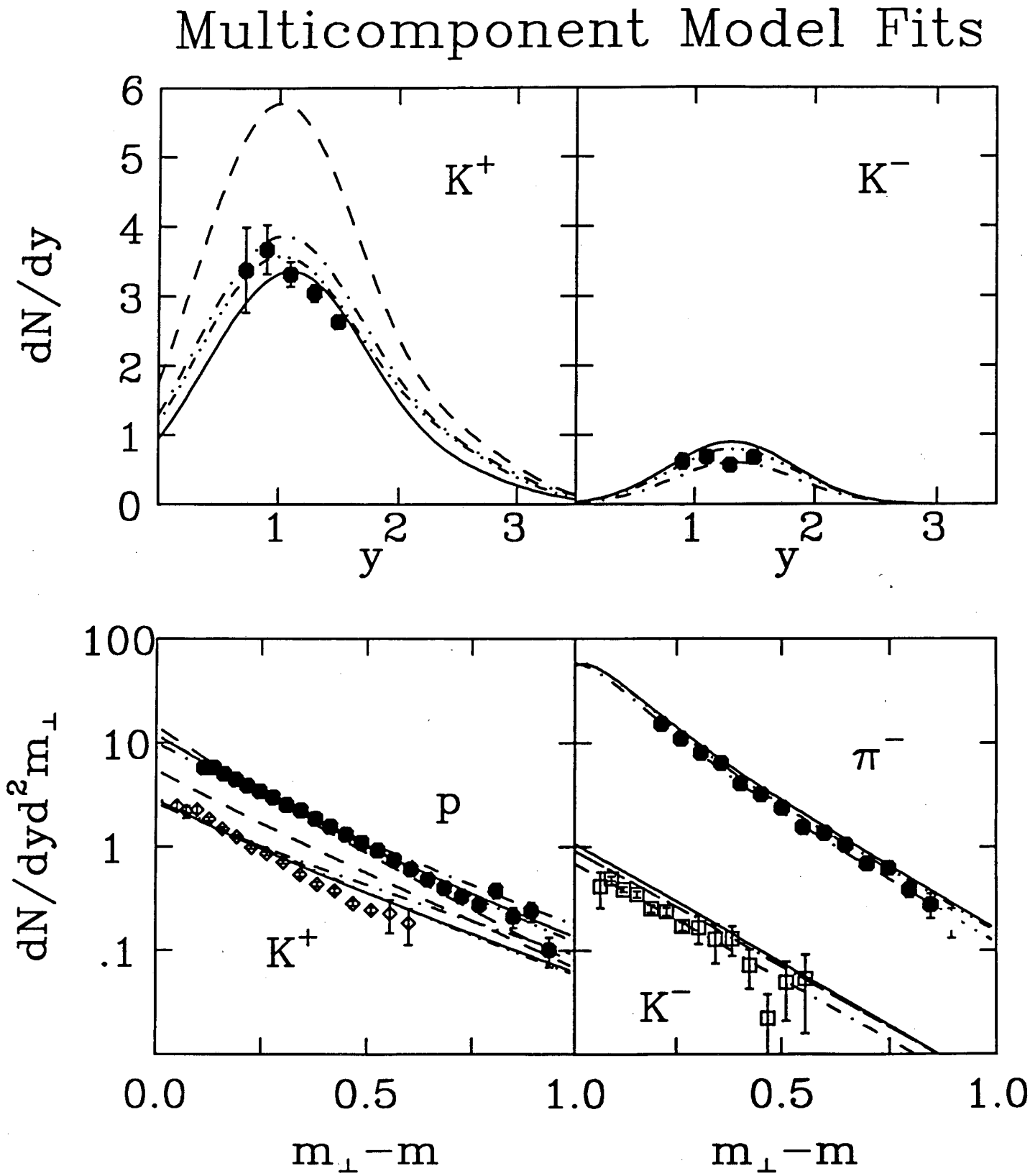

Fig. 11 p. 35

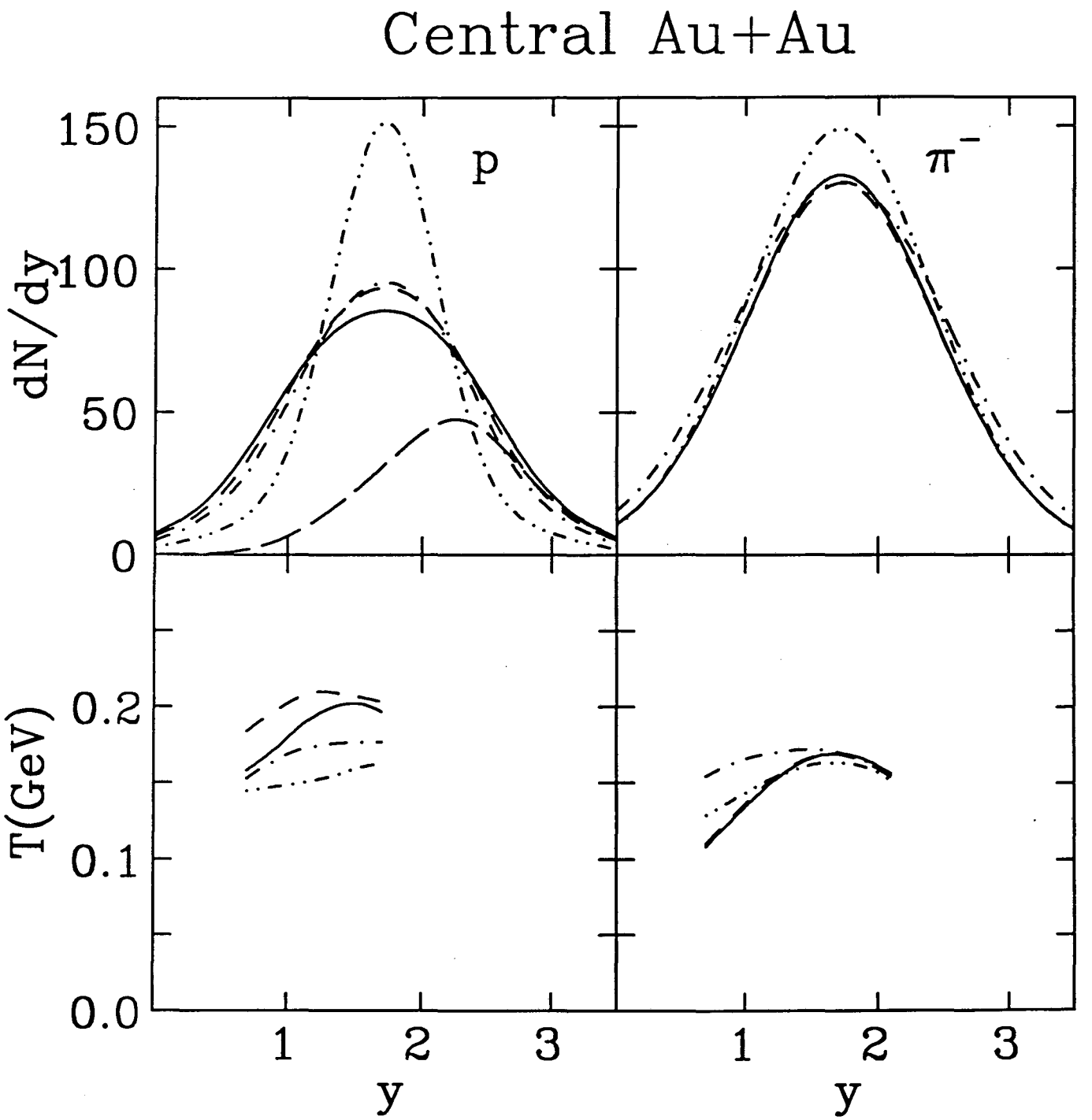

Fig. 12 p. 36

LAWRENCE BERKELEY LABORATORY
UNIVERSITY OF CALIFORNIA
INFORMATION RESOURCES DEPARTMENT
BERKELEY, CALIFORNIA 94720